



Probing the Specificity of the S₁ Binding Site of Subtilisin Carlsberg with Boronic Acids†

Peter Seufer-Wasserthal, Valeri Martichonok, Thomas H. Keller, Bain Chin, Richard Martin
 and J. Bryan Jones*

Department of Chemistry, University of Toronto, Lash Miller Laboratories, 80 St George Street, Toronto,
 Canada M5S 1A1

Abstract—A range of aryl and arylalkyl boronic acids has been prepared and evaluated as inhibitors of the serine protease subtilisin Carlsberg, with the goal of exploring the factors controlling binding to the S₁ site.

Introduction

Enzymes are now widely used for asymmetric synthetic transformations in organic chemistry.¹ However the factors responsible for determining the structural and stereospecificity of enzymes towards unnatural substrates and inhibitors remain poorly understood. Among the interactions generally considered as contributors to, or opposing, binding are steric effects, electrostatic and hydrogen bonds, hydrophobic effects arising from solvent reorganization, and stacking interactions.² We became interested in this area because identifying and understanding the factors controlling substrate and inhibitor binding is an essential prerequisite for the selection of enzymes best suited to cope with the increasingly broad structural range of substrates imposed by the chiral synthon demands of asymmetric synthesis.³ As one step in this direction, we recently began to analyze the binding of selected substrates and inhibitors to synthetically useful proteases. This was approached using a combination of enzyme kinetics and molecular modeling,⁴ with the ultimate goal of identifying and understanding the active site interactions involved and with a view to eventually formulating guidelines for predicting binding affinities and orientations for any new, unnatural, substrate and inhibitor structures with synthetically useful enzymes.

Subtilisin Carlsberg (EC 3.4.21.14) was chosen as the initial enzyme vehicle for these studies, being a commercially available serine protease that has been applied synthetically⁵ and for which a high resolution X-ray crystal structure is available.⁶ While a considerable amount of kinetic data has been accumulated for this enzyme,⁷ the published data represent an unsatisfactory basis for forecasting the behavior of new substrates because

of the somewhat haphazard range of literature structures surveyed and of the wide variations in the assay conditions applied. Subtilisin Carlsberg has an extended binding region composed of several subsites of which the S₁-pocket⁸ is of greatest current relevance to the preparation of chiral synthons. Delineation of the features controlling binding to the S₁-pocket, and of the structural and electrostatic properties of substrates that promote good S₁-interactions, is thus of primary importance.

For systematic probing of enzyme specificity, evaluating the binding affinities of competitive inhibitors represents a convenient strategy. It is this approach that is followed in this paper, using a structurally coherent range of boronic acid inhibitors. Boronic acids are generally very effective reversible, transition state, inhibitors of serine proteases⁹ and of subtilisin Carlsberg in particular, as a preliminary study has confirmed.¹⁰ In this paper, we continue our exploration of the dimensions, steric tolerance, and electrostatic properties, of the generally hydrophobic S₁ binding pocket of subtilisin Carlsberg using the boronic acid inhibitors RB(OH)₂ 1–32, possessing the range of different R-groups identified in Tables 1 and 2.

Results and Discussion

Preparation of boronic acids

The boronic acids used for this study were purchased or were prepared as shown in Scheme I from commercially available carboxylic acid starting materials. In the first step of each boronic acid preparation, the precursor bromide was reacted with activated magnesium to give the corresponding Grignard reagent, which was slowly added with vigorous stirring to a mixture of trimethyl borate in ether at low temperature. As noted in the literature,¹¹ the yield of this reaction is highly dependent on the reaction temperature and the stirring speed. In this regard we found that the best results were achieved with mechanical stirring at 500–1000 rpm. The boronic acids obtained in this step are contaminated with borinic acids. The rate of formation of borinic acid versus boronic acid was found to depend on the

†This paper is dedicated to Professor Charlie Sih in honor of his 60th birthday, to recognize his giant and seminal contributions to the field of enzymes in organic synthesis, and to acknowledge his friendship, help and encouragement given so generously over many years (to JBJ).

Keywords—Serine protease, subtilisin Carlsberg, S₁ pocket, boronic acid, inhibition, probing determinants of enzyme specificity.

Table 1. Inhibition of subtilisin Carlsberg by phenylboronic acids 1–13^a

Inhibitor RB(OH) ₂	R	K _i (μM)	1/K _{bind} (μM)
1		100 ± 3	23.0
2		7 ± 0.8	1.1
3		56 ± 4	8.4
4		23 ± 1	1.9
5		180 ± 10	31
6		8 ± 0.7	0.008
7		75 ± 5	.b
8		12 ± 1.2	1.2
9		10 ± 0.8	1.9
10		6 ± 1.2	1.1
11		4 ± 0.8	0.40
12		2 ± 0.3	0.38
13		37 ± 2	0.41

^aK_i values were determined in duplicate at pH 7.1 in 0.1 M phosphate buffer and 25 °C. Initial rates were measured at substrate (TAME) concentrations in the range of 0.015–0.30 M, inhibitor concentration 10⁻⁶–10⁻³ M and enzyme concentration 3.7 × 10⁻⁷ M.

^bEstimation of K_{bind} not possible due to unavailability of experimental ΔG_{desolv} value for aniline.

Table 2. Inhibition of subtilisin Carlsberg by alkyl and arylalkyl boronic acids 14–32^a


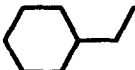
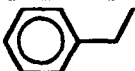
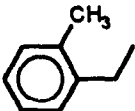
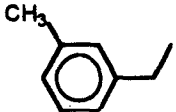
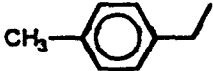
Inhibitor RB(OH) ₂	R	K _i /μM	1/K _{bind} (μM)
14	CH ₃	$1.3 \times 10^4 \pm 1.3 \times 10^3$	_b
15		$1.3 \times 10^3 \pm 200$	2.8×10^4
16		$3.3 \times 10^3 \pm 400$	2.6×10^4
17		257 ± 19	59
18		520 ± 21	114
19		225 ± 8	50
20		270 ± 15	59

Table 2. *Continued*

21		525 ± 28	89
22		296 ± 14	50
23		58 ± 4	9.9
24		48 ± 3	.C
25		684 ± 70	103
26		94 ± 7	14
27		19 ± 1	2.9
28		202 ± 20	7.7×10^3 ^d
29		360 ± 21	.b
30		110 ± 4	2.0
31		120 ± 8	2.2
32		$2.7 \times 10^3 \pm 400$.C

^a K_i values were determined in duplicate at pH 7.1 in 0.1 M phosphate buffer and 25 °C. Initial rates were measured at substrate (TAME) concentrations in the range of 0.015–0.30 M, inhibitor concentration 10^{-6} – 10^{-3} M and enzyme concentration 3.7×10^{-7} M.

^bNot estimated since K_i value so high.

^cEstimation of K_{bind} not possible due to unavailability of experimental ΔG_{desolv} values for the corresponding substituted benzenes.

^dThe free energy of desolvation of trifluoromethylbenzene of -2.16 kcal/mole was estimated from bond and group contributions as described in Ref. 20(b).

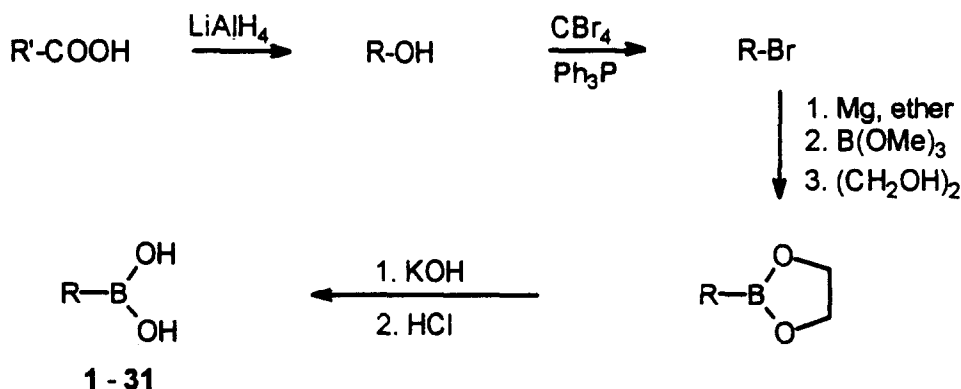
nature of the trialkyl boronate used, with trimethyl borate being the most satisfactory. For example, in the preparation of phenylboronic acid (**1**) borinic acid formation is negligible with trimethyl borate as the boron source but rises to a 25% yield when tributyl borate is used.¹² Accordingly, trimethyl borate was used in all current preparations. Isolation of the boronic acids as their cyclic ethylene glycol esters permitted facile purification by distillation.¹³ Subsequent hydrolysis then gave **5**, **8**, **10**, **11**, **13**, **16–31** in a crystalline form suitable for direct use in the enzyme kinetic studies. The 2-(4-carboxyphenyl)ethyl boronic acid (**32**) was prepared by the route outlined in Scheme II in which methyl 4-hydroxy benzoate (**33**) was converted to the triflate **34**, followed by Stille coupling¹⁴ with tetravinyltin to yield **35**, which on treatment with dibromoborane–dimethyl sulfide¹⁵ gave the boronic acid **32** in 12% overall yield.

While pure boronic acids are usually air-stable, freshly prepared samples may undergo autoxidation. Such

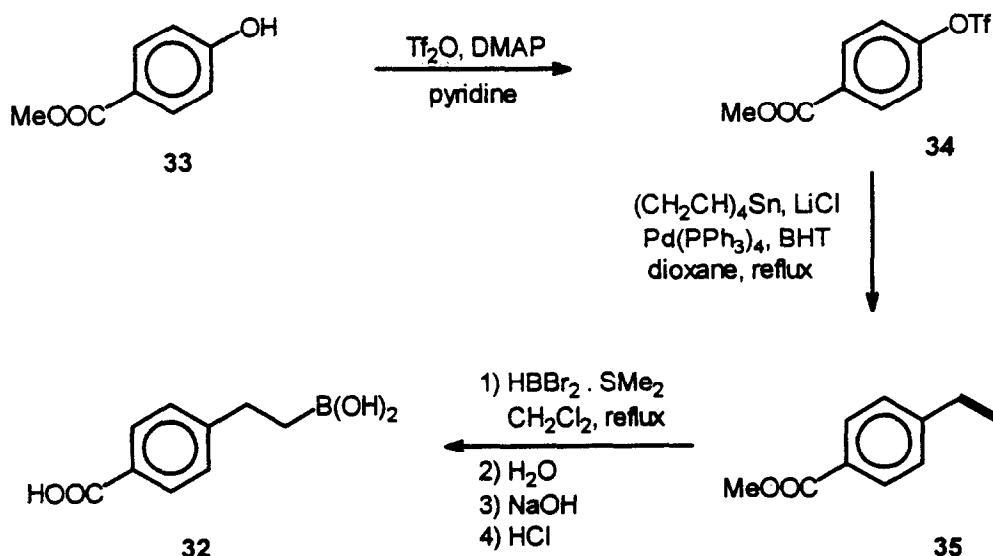
autoxidation is inhibited by water. Accordingly, all the boronic acids in this study were stored at 0 °C without drying. Similarly, the purchased boronic acids **1–4**, **6**, **7**, **9**, **12**, **14**, **15** were recrystallized from aqueous solution prior to use.

Inhibition studies

For the kinetic determinations, the inhibitors **1–32** were divided into two groups on the basis of structural similarities, with the phenylboronic acid **1–13** and alkyl and arylalkyl boronic acid **14–32** categories being the most clearly distinguishable. The individual inhibition constants for each inhibitor for subtilisin Carlsberg were determined using a pH-stat method and with *N*-para-tosyl-L-arginine methyl ester (TAME) as the standard reference substrate.³ Each boronic acid was found to be a competitive inhibitor and the results are summarized for **1–13** and **14–32** in Tables 1 and 2 respectively.



Scheme I.



Scheme II.

Inhibition by phenylboronic acids 1–13

The phenylboronic acids 1–13 were all excellent inhibitors (Table 1). A pattern of substituent effects on K_I is immediately evident in that electron withdrawing substituents enhance, and electron donating substituents decrease, the binding affinity of a phenylboronic acid to subtilisin Carlsberg. For example, a 60-fold difference in K_I was manifest between the *para*-methoxy and 3,5-dichloro substituent effects of inhibitors 5 and 12, respectively. While this indicates that the efficacies of the phenylboronic acids 1–13 as competitive inhibitors reflect, at least in part, the differences in the electrophilicities of the individual boron atoms, no linear relationship was evident when the K_I values of Table 1

were plotted in a Hammett-like manner against the σ parameters of the substituents. Thus the relative capacities of these compounds to inhibit subtilisin Carlsberg cannot be explained simply in terms of the influence of a given substituent on the electrophilicity of the boron, and hence of the strength of the boron atom interaction with the active site serine nucleophile. On the other hand, for the monosubstituted boronic acids 1–6, a plot of the $-pK_a$ values,¹⁶ which directly reflect the influence of boron electrophilicity on acidity, against σ gave a good linear correlation (Figure 1(a)), whose ρ value of 2.04 ± 0.09 is in good agreement with the literature value.¹⁷ The apparent contradiction between the K_I vs σ and $-pK_a$ vs σ plots is attributed to solvation effects, which always play a major role in determining enzyme–inhibitor binding strengths.

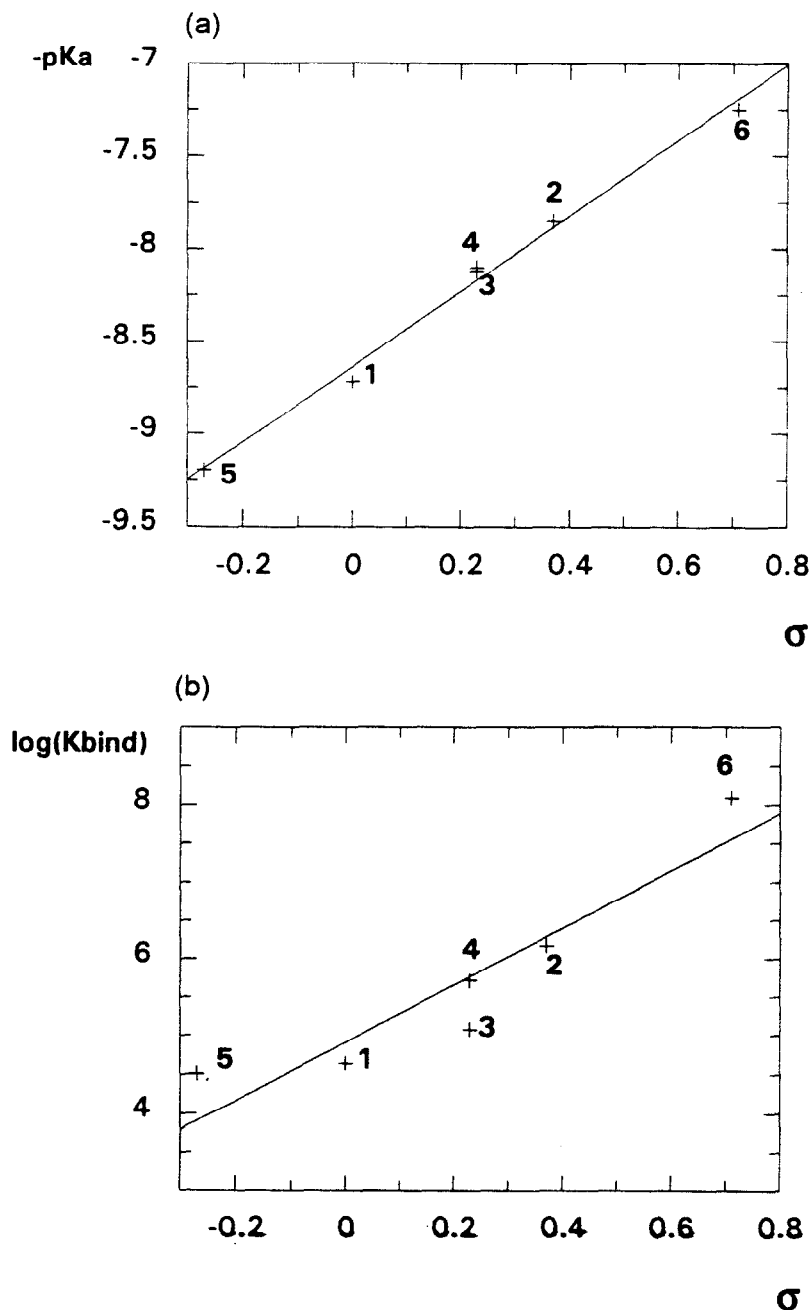


Figure 1. Hammett plot correlations of the effects of substituents on (a) the pK_a -values of phenylboronic acids and (b) the solvation-corrected inhibition constant $1/K_{bind}$ for phenylboronic acid inhibition of subtilisin Carlsberg. Substituents are H(1), *m*-Cl (2), *p*-Cl (3), *p*-Br (4), *p*-OMe (5) and *m*-NO₂ (6)

Unfortunately, reliable general methods for the quantitative evaluation of the contributions of solvation–desolvation processes in EI-formation remain elusive. Nevertheless, we have attempted to take solvation effects into account using the following protocol.

When it binds to a protein, an inhibitor must be removed, at least in part, from solvent water. If an inhibitor is very hydrophobic, the effect of squeezing the molecule out of the aqueous phase into a hydrophobic pocket can be very important.¹⁸ Although phenylboronic acids are too small to fit optimally into the S₁ binding site, molecular graphics analysis shows that phenyl rings themselves must be stripped of water in the EI-complex. By extension of the Wolfenden concept,^{18b} we have characterized the steps involved in binding in terms of an equilibrium constant, $K_{\text{desolv(ation)}}$, of partial desolvation and of an equilibrium constant, $K_{\text{bind(ing)}}$, for binding to the enzyme of a partially desolvated inhibitor. This situation is depicted in Figure 2. K_{bind} represents a measure of the "true" affinity of the inhibitor for the enzyme in that it is free from solvent effects. The equilibrium constant of desolvation, K_{desolve} can be calculated from the free energy of desolvation, ΔG_{desolv} . We attempted to calculate the solvation energies involved for binding of 1–13 using Biosym's DelPhi¹⁹ program but the results were ambiguous, and inconsistent with marker experimental values. Fortunately, free energies of desolvation have been evaluated for many compounds from their water-to-vapor distribution coefficients.²⁰ Accordingly, this latter method was applied in all solvation–desolvation calculations in the current study, with the exception of the trifluoromethyl derivative **28**, for which the experimental data needed are unavailable. Fortunately, however, to a reasonable approximation, the contributions of the constituent groups of a compound to its ΔG_{desolv} value are additive, and the solvation energies derived in this way are generally consistent with experimental values.²⁰ Accordingly, this strategy was applied to estimate ΔG_{desolv} for **28**.

In the current study, we have made the assumption that the partial free energies of desolvation (ΔG_{desolv}) for inhibitors 1–13 are equal to the desolvation energies of the corresponding substituted benzenes. Based on the Figure 2 equation, K_I can be re-expressed as $1/K_{\text{bind}}K_{\text{desolv}}$, or $1/K_{\text{bind}} = K_I/K_{\text{desolv}} = K_I/e^{-\Delta G_{\text{desolv}}/RT}$. The values of $1/K_{\text{bind}}$, which may be considered the "true" inhibition

constants, calculated from literature^{20b} values for ΔG_{desolv} and the current K_I data are recorded in Table 1. From these values it can be seen that, for each inhibitor 1–13, the free energy of desolvation represents a negative binding contribution. Now, a Hammett-plot for 1–6 of $\log(K_{\text{bind}})$ vs σ gives a ρ value of 3.76 ± 0.75 (Figure 1(b)). The combined Figure 1 data thus show that substituent groups that withdraw electron density from the boron atom of phenylboronic acids will stabilize the adducts of boronic acids with OH^- , and with the enzyme's active site serine hydroxyl group in the tetrahedral EI-complex, in an analogous manner. The positive ρ values observed in both plots demonstrate that the negatively charged species formed in titration of a phenylboronic acid with hydroxide, and in subtilisin Carlsberg inhibition, are similar in character. The higher ρ value for the enzyme plot reflects the greater charge separation in a tetrahedral boronic acid–subtilisin Carlsberg complex, involving a positively charged histidine imidazolium group and the oxyanion hole, than in the corresponding boronic acid–hydroxide ion adduct, which is stabilized by water only. On another aspect of EI-binding, the lower K_I for 3-biphenylboronic acid (**13**) than for the phenylboronic acid (**1**) parent can be attributed to a better fit of a biphenyl residue than a phenyl group into the hydrophobic S₁ pocket.

Inhibition by alkyl and arylalkylboronic acids (14–32)

The competitive inhibition constants for the inhibition of subtilisin Carlsberg by the boronic acids **14–32** are recorded in Table 2 together with the calculated values of $1/K_{\text{bind}}$ that take solvation–desolvation into account. While methylboronic acid (**14**), the smallest possible boronic acid, is a very poor inhibitor of subtilisin Carlsberg its K_I value is interesting since it provides a measure of the contribution that the active site serine221-to-boronic acid addition itself makes to inhibitor binding, devoid of the additional binding stabilization bestowed by the side chains of **15–32** with active site regions such as S₁. Alkylboronic acids are generally worse inhibitors of serine proteases than arylboronic acids,²¹ a pattern confirmed by comparison of the inhibition constants of the other two alkylboronic acids **15** and **16** with the Table 1 values. While **15** and **16** do have lower K_I 's than **14**, they are still poor inhibitors.

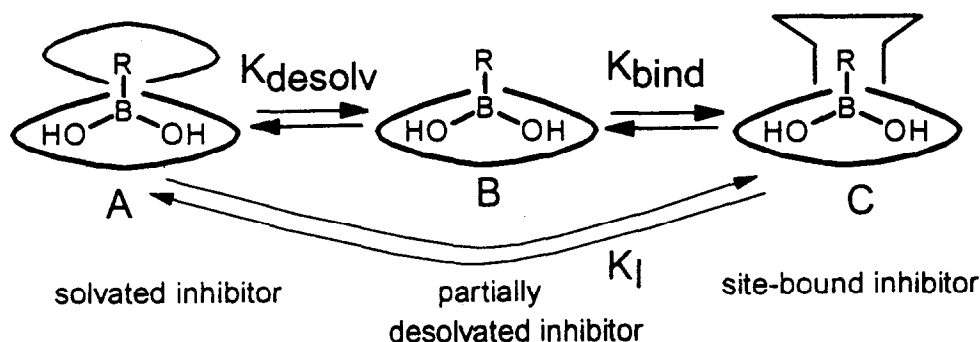


Figure 2. Solvation–desolvation steps envisaged in binding of boronic acids to subtilisin Carlsberg

The change in inhibition constant on replacing the cyclohexyl ring of **16** with a phenyl group, as in **17**, is dramatic, with the K_I of 2-phenylethylboronic acid (**17**) being 128-fold lower, at 270 μM . There is little change in the inhibition constant if the aromatic ring of **17** is substituted with methyl groups in either the *meta*- (**18**) or *para*-position (**19**), or by a *meta*-methoxy group, as in **22**. Chain extension by one CH_2 -group also has minimal effect, with the K_I 's of **17** and **29** remaining close. In contrast, *ortho*-substitution of **17** is detrimental, with compounds **18**, **21**, and **25** exhibiting K_I 's ~ 2 -fold higher than that of the unsubstituted parent **17**. This is indicative of steric crowding in the upper part of the S_1 binding pocket. In contrast, electronegative substituents in the *para*-position contribute very positively to inhibitor binding, as exemplified by the low K_I 's of 4-methoxy-, 4-fluoro- and 4-chlorophenylethylboronic acids **23**, **24** and **27** respectively. In fact, the K_I of **19** μM for **27** is the lowest of all the Table 2 inhibitors. Introduction of a naphthyl group, as in **31** and **32**, also improves binding ~ 2 -fold relative to the phenylethylboronic acid standard. On the other hand, the electron withdrawing 4-trifluoromethyl- and 4-carboxy substituents did not exert the same beneficial effect on binding. While inhibition by **28** was marginally better than that of **17**, introduction of the *para*-carboxy substituent, as in **32**, created a very poor inhibitor whose K_I of 2.7 mM matches those of the alkylboronic acids **14**–**16**.

Applications of molecular graphics analyses in conjunction with molecular dynamics and electrostatic potential calculations permitted the data of Table 2 to be interpreted more completely. The X-ray structure of subtilisin Carlsberg⁶ was energy-minimized using the Biosym "Discover" program and the boronic acid inhibitors **14**–**32** then individually docked into the active site. Each EI-complex was then subjected to energy-minimization by Discover's molecular mechanics protocol, followed by molecular dynamics simulation for 20 ps.

Analyses of the trajectories showed that the phenylethylboronic acids oriented themselves at the active site such that, for the two hydroxyl groups attached to the boron atom, the oxygen atom of one forms a hydrogen bond of length $2.4 \pm 0.2 \text{ \AA}$ to Ne of His64 and the oxygen of the other forms a hydrogen bond to the amide hydrogens of Asn155 of the oxyanion hole. The phenyl ring remains in the S_1 pocket after the molecular dynamics simulation.

The S_1 pocket of the enzyme is too narrow to permit the cyclohexane ring of **16** to fit satisfactorily, despite the driving force of a highly favorable desolvation effect, nor to allow good binding of the *ortho*-substituted compounds **18**, **21**, and **25**. However, the S_1 groove is long enough to accommodate with ease phenylethylboronic acid (**17**), the *para*- and *meta*-substituted compounds **19**, **20**, **22**–**24**, **26**–**28**, and **32**, the naphthyl derivatives **30** and **31**, and 3-phenylpropylboronic acid (**29**). Interestingly, although 2-(4-methylphenyl)ethylboronic acid (**20**) and 2-(4-trifluoromethylphenyl)ethylboronic acid (**28**) are structurally and sterically similar, their binding affinities

differ by 130-fold when the desolvation effects are taken into consideration. This can be accounted for by the capacity of aromatic rings to act as hydrogen-bond acceptors.²² In this regard, the S_1 pocket of subtilisin Carlsberg is lined by the backbone atoms of Gly154 and Asn155 on one side, by Leu126, Gly127 and Gly128 on the other, and by Gly166 and Tyr167 at the bottom. The hydrogen atoms of peptide bond nitrogens of these residues represent sites for potential hydrogen bonding to the aromatic rings of appropriate Table 2 inhibitors. This accounts for the excellent binding of the electron-rich naphthylboronic acids **30**, **31** and the 4-methoxy compound **23**. It also explains the better binding of the more electron rich 2-methoxy- (**21**) than 2-methyl- (**18**) and 2-chlorophenylethylboronic acid (**25**). The poor inhibitory properties of **28** are now rationalizable in terms of the deleterious effect on S_1 hydrogen bonding resulting from the low electron density induced in the aromatic ring of **28** by the *para*-trifluoromethyl substituent which, furthermore, is itself a poor hydrogen-bond acceptor.

Contributions of electrostatic attractions to EI-binding were also investigated. Calculations using the DelPhi program of the electrostatic potential²³ of the active site region of subtilisin Carlsberg identified regions of positive charge located on both sides of S_1 and in proximity to Gly128, Ala129 and Tyr167 at, and beyond, the bottom of the S_1 pocket. This is evident in Figure 3, which depicts the EI-complex of the enzyme with the excellent inhibitor **27**. The negative potential of the *para*-chloro group of **27** overlaps with the positive region at the bottom of S_1 to give a beneficial electrostatic contribution to EI-binding. Such overlap turns out to be generally advantageous. Comparative calculations on the EI complexes of subtilisin Carlsberg with **17**, **24** and **27** revealed that the lowering of K_I 's induced by the introduction of a *para*-fluoro- or chloro substituent were attributable to electrostatic attractions between the negative potential of the fluoro or chloro function of the inhibitor with the positive potential on the enzyme's surface adjacent to the bottom of the S_1 pocket. In the minimized EI-complexes of **24** and **27**, the electronegative *para*-fluoro and chloro-substituents respectively point to the bottom of S_1 where they are attracted to the partially positively charged hydrogen atoms attached to the peptide-bond nitrogen atoms of Tyr167, Ala129 and Gly128. The same effect is evident in the better binding than **17** of the *meta*-chloro inhibitor **26**. Disappointingly, 2-(4-carboxyphenyl)ethylboronic acid (**32**), whose *para*-carboxyl function was designed to interact, in its carboxylate conjugate base form, with the positive region emanating from the rear of S_1 , was a very poor inhibitor. We attribute this to the very high free energy cost of desolvation involved in transferring a carboxylate group out of aqueous solution into a hydrophobic active site pocket.²⁴

While the current results represent only a first step towards exploring the factors controlling binding to the S_1 groove of subtilisin Carlsberg, they have identified several factors that can contribute to good binding. Future studies will probe these aspects further.

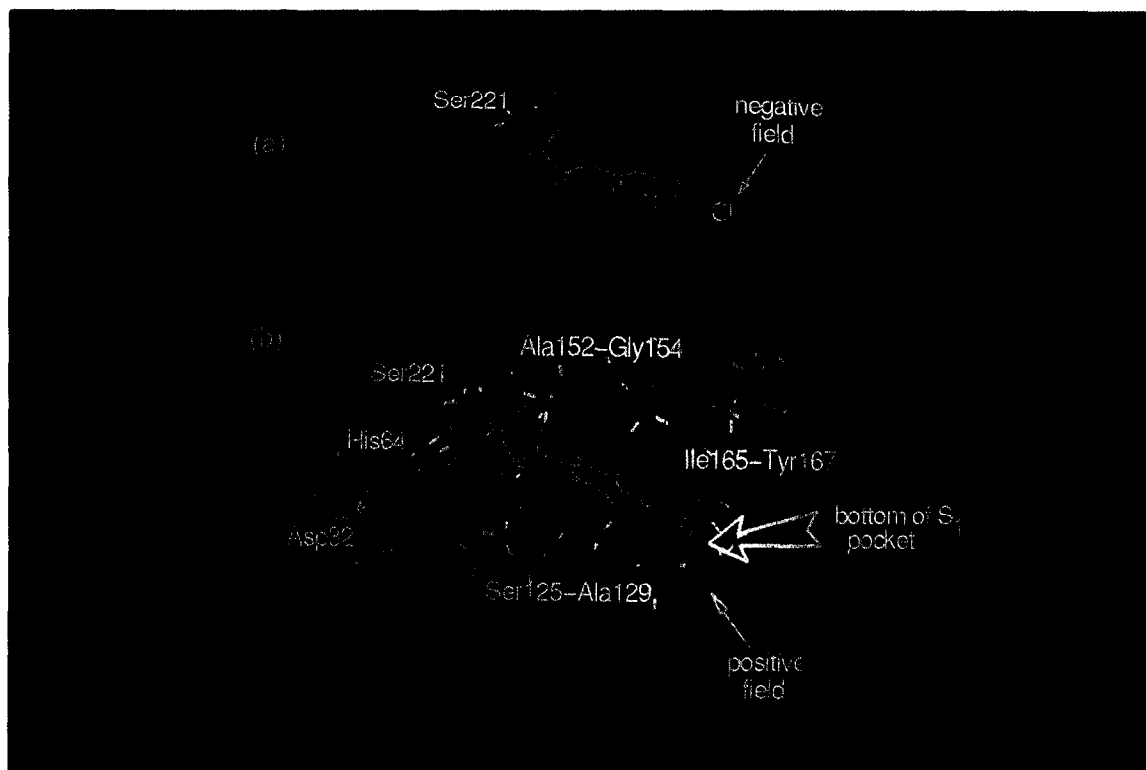


Figure 3. Electrostatic contribution to inhibitor binding in the S₁ pocket. Isocontours were obtained at -20 kcal/mole for both positive (blue) and negative (red) electrostatic potentials. (a) The *DelPhi* calculated electrostatic potential for 2-(4-chlorophenyl)ethylboronic acid (27) shows the large negative potential associated with the *para*-chloro group (identified by the arrow \leftarrow). (b) The tetrahedral EI-complex of subtilisin Carlsberg and 27 is shown. The electrostatic potential surface of the enzyme is depicted, with the inhibitor structure in line-form only for clarity. The region extending beyond the bottom of the S₁ pocket is seen to be one of positive potential (blue, identified by arrow \leftarrow) with which the negative field of the *para*-chloro can interact in an electrostatically attractive manner. The extent of this overlap can be envisaged by mental juxtaposition of the (a) and (b) images

Experimental Section

General methods

Unless otherwise stated, all reactions were performed under nitrogen using oven-dried glassware. Anhydrous reagents were prepared according to literature procedures.²⁵ Preparative flash column chromatography was performed using silica gel 60 (40–63 μ), supplied by Toronto Research Chemicals Inc. Melting points were obtained on a Tottoli melting point apparatus, and are uncorrected. Boiling points are uncorrected. IR spectra were determined in KBr pellets (for solids) and films (for liquids) on a Nicolet 5DX FTIR spectrophotometer. NMR (¹H, ¹³C) spectra were recorded on a Gemini 200 (200 MHz, 50 MHz respectively) spectrometer unless otherwise indicated. ¹H NMR chemical shifts are reported in ppm relative to the CHCl₃ peak (δ = 7.24) with CHCl₃ as solvent; the DMSO peak (δ = 2.49) in DMSO-*d*₆ and the HOD peak (δ = 4.80) in D₂O. ¹³C NMR chemical shifts are reported in ppm relative to the CHCl₃ peak (δ = 77.00) with CHCl₃ as solvent, the DMSO peak (δ = 39.50) in DMSO-*d*₆ and relative to external dioxane (δ = 66.50) in D₂O as solvent. Mass spectra were measured on a Bell and Howell 21-490 (low resolution) or AEI MS3074 instrument (high resolution).

Dibromoborane, bromobenzene, 4-bromoanisole, 2,3-dichloro-1-bromobenzene, 2,5-dichloro-1-bromobenzene and 3,4-dichloro-1-bromobenzene, (2-bromoethyl)benzene, 2-(4-fluorophenyl)ethanol, 1-bromo-3-phenylpropane, 2-methylphenylacetic acid, 3-methylphenylacetic acid, 4-methylphenylacetic acid, 2-methoxyphenylacetic acid, 3-methoxyphenylacetic acid, 4-methoxyphenylacetic acid, 4-trifluoromethylphenylacetic acid, 4-chlorophenylacetic acid, 1-naphthylacetic acid, 2-naphthylacetic acid, 2-(4-fluorophenyl)ethanol, 2-cyclohexylethanol, phenylboronic acid (1), 4-bromophenylboronic acid (4), 3-nitrophenylboronic acid (6), 3-aminophenylboronic acid (7) and methylboronic acid (14) were obtained from Aldrich. 4-Chlorophenylboronic acid (3), 2,4-dichlorophenylboronic acid (9) and 3,5-dichlorophenylboronic acid (12) were purchased from Lancaster and methyl 4-hydroxy benzoate (33) from Baker. *n*-Butylboronic acid (15) and subtilisin Carlsberg (Lot 29F-0050) were obtained from Sigma. (2-Bromoethyl)-cyclohexane, 1-(2-bromoethyl)-2-methylbenzene, 1-(2-bromoethyl)-3-methylbenzene, 1-(2-bromoethyl)-4-methylbenzene, 1-(2-bromoethyl)-2-methoxybenzene, 1-(2-bromoethyl)-3-methoxybenzene, 1-(2-bromoethyl)-4-methoxybenzene, 1-(2-bromoethyl)-2-chlorobenzene, 1-(2-bromoethyl)-3-chlorobenzene, 1-(2-bromoethyl)-4-chlorobenzene, 1-(2-bromoethyl)-4-trifluoromethylbenzene, 1-(2-bromoethyl)naphthalene, 2-(2-bromoethyl)naphthalene and 3-bromobiphenyl were

prepared from the corresponding alcohols. The alcohols were conveniently prepared by reduction of the corresponding acids with LiAlH_4 . 3-Chlorophenylboronic acid (**2**) and 3,5-dichlorophenylboronic acid (**12**) were gifts from Professor H. Hönig.

General procedure for preparation of boronic acids

The method for 4-methoxyphenylboronic acid (**5**) is representative.

4-Methoxyphenylboronic acid (5). 4-Methoxyphenylmagnesium bromide was prepared from magnesium (1.46 g, 0.06 mol) and 4-bromoanisole (6.26 mL, 0.05 mol) in ether (75 mL). This solution was added during the course of 1 h to a solution of trimethyl borate (5.88 mL, 0.05 mol) in dry diethyl ether (150 mL). The reaction mixture was mechanically stirred and cooled so that the internal temperature was maintained below -60°C . After all the Grignard reagent had been added, the white suspension was allowed to warm slowly (preferably overnight) to room temperature. The reaction mixture was then added slowly to 10% aqueous H_2SO_4 (50 mL) at 0°C . The ether layer was separated and the aqueous phase extracted with ether (3 x 50 mL). The combined organic phases were dried (MgSO_4), filtered, added to a flask containing ethylene glycol (3.10 g, 0.05 mol) and stirred vigorously for 30 min. After addition of hexanes (200 mL) the aqueous phase was separated and the organic layer dried (MgSO_4) and filtered. Evaporation of the solvents and distillation furnished the desired ethylene glycol boronate, which was dissolved in ether (50 mL) and extracted with 1 M aqueous KOH (5 x 30 mL). The combined aqueous layers were washed with diethyl ether (30 mL) and acidified to pH 1 with 10% hydrochloric acid. The precipitated boronic acid was then extracted into diethyl ether (5 x 30 mL) and the combined ether layers washed with saturated aqueous NaCl. The organic phase was added to water (25 mL) and the volatile components of the two phase mixture removed at $\leq 30^\circ\text{C}$ on a rotary evaporator until 5 mL of water had distilled into the receiver. The remaining mixture was then cooled at 4°C for 2 h and the crystalline boronic acid collected by filtration and stored under argon. The product **5** (3.50 g, 46% yield after recrystallization from water) had m.p. $155\text{--}157^\circ\text{C}$. IR (KBr) $3600\text{--}3000$, 1650 , 1570 , 1350 , 780 cm^{-1} . ^1H NMR δ (DMSO- d_6) 3.42 (3H, s), 6.88 (2H, d, $J = 8.5\text{ Hz}$), 7.74 (2H, d, $J = 8.5\text{ Hz}$), 7.85 (2H, s, exchangeable with D_2O). ^{13}C NMR (CDCl_3) δ 54.9 , 113.2 , 136.2 , 161.4 . HRMS 402.1570 (calcd for anhydride $\text{C}_{21}\text{H}_{21}\text{B}_3\text{O}_6$: 402.1617).

The other boronic acids were prepared analogously,²⁶ as follows.

2,3-Dichlorophenylboronic acid (8). 38% yield from 2,3-dichloro-1-bromobenzene, m.p. $241\text{--}242^\circ\text{C}$. IR (KBr) $3600\text{--}2800$, 1522 , 1411 , 1365 , 1004 , 979 , 792 , 690 cm^{-1} . ^1H NMR (DMSO- d_6) δ $7.25\text{--}7.35$ (2H, m), $7.5\text{--}7.6$ (1H, m), 8.49 (2H, s, exchangeable with D_2O). ^{13}C NMR (DMSO- d_6) δ 128.8 , 131.7 , 132.7 , 134.2 , 139.7 . HRMS 189.9764 (calcd for anhydride $\text{C}_6\text{H}_5\text{BCl}_2\text{O}_2$: 189.9760).

2,5-Dichlorophenylboronic acid (10). 49% yield from 2,5-dichloro-1-bromobenzene, m.p. $202\text{--}203^\circ\text{C}$. IR (KBr) $3600\text{--}2800$, 1550 , 1252 , 1005 , 787 cm^{-1} . ^1H NMR (DMSO- d_6) δ $7.3\text{--}7.4$ (2H, m), $7.8\text{--}7.9$ (1H, m), 8.45 (2H, s, exchangeable with D_2O). ^{13}C NMR (DMSO- d_6) δ 130.2 , 130.7 , 131.6 , 133.4 , 135.0 . HRMS 515.8982 (calcd for anhydride $\text{C}_{18}\text{H}_9\text{B}_3\text{Cl}_6\text{O}_3$: 515.8962).

3,4-Dichlorophenylboronic acid (11). 63% yield from 3,4-dichloro-1-bromobenzene, m.p. $275\text{--}277^\circ\text{C}$. IR (KBr) $3600\text{--}2800$, 1551 , 1250 , 1005 , 979 , 788 cm^{-1} . ^1H NMR (DMSO- d_6) δ $7.4\text{--}7.8$ (3H, m), 7.95 (2H, s, exchangeable with D_2O). ^{13}C NMR (DMSO- d_6) δ 130.6 , 131.5 , 133.8 , 134.8 , 136.5 . HRMS 515.8976 (calcd for anhydride $\text{C}_{18}\text{H}_9\text{B}_3\text{Cl}_6\text{O}_3$: 515.8962).

3-Biphenylboronic acid (13). 18% yield from 3-biphenylbromide; m.p. $202\text{--}204^\circ\text{C}$ (lit.²⁷ m.p. $207\text{--}208^\circ\text{C}$). IR (KBr) $3600\text{--}3000$, 1550 , 1005 , 979 cm^{-1} . ^1H NMR (DMSO- d_6) δ $7.3\text{--}8.2$ (m). ^{13}C NMR (DMSO- d_6) δ 126.9 , 127.5 , 128.3 , 128.6 , 129.2 , 132.8 , 133.5 , 139.5 , 140.9 .

2-Cyclohexylethylboronic acid (16). 43% yield from (2-bromoethyl)cyclohexane, m.p. $88\text{--}89^\circ\text{C}$. IR (KBr) $3300\text{--}3000$, 2923 , 1549 , 1376 , 1224 , 1004 , 979 cm^{-1} . ^1H NMR (DMSO- d_6) δ $0.35\text{--}1.25$ (10H, s), $1.5\text{--}1.8$ (5H, m), 7.31 (2H, s, exchangeable with D_2O). ^{13}C NMR (DMSO- d_6) δ 12.4 (broad), 25.9 , 26.4 , 31.8 , 32.7 , 39.5 . HRMS 414.3648 (calcd for anhydride $\text{C}_{24}\text{H}_{45}\text{B}_3\text{O}_3$: 414.3665).

2-Phenylethylboronic acid (17). 55% yield from (2-bromoethyl)benzene, m.p. $85\text{--}87^\circ\text{C}$ (lit.²⁷ m.p. 88°C). IR (KBr) $3500\text{--}3200$, 1377 , 1039 , 695 cm^{-1} . ^1H NMR (DMSO- d_6) δ 0.90 (2H, t, $J = 8\text{ Hz}$), 2.62 (2H, t, $J = 8\text{ Hz}$), $7.1\text{--}7.3$ (5H, m), 7.53 (2H, s, exchangeable with D_2O). ^{13}C NMR (DMSO- d_6) δ 18.6 (broad), 32.3 , 128.7 , 130.8 , 131.6 , 147.8 . HRMS 396.2220 (calcd for anhydride $\text{C}_{24}\text{H}_{27}\text{B}_3\text{O}_3$: 396.2230).

2-(2-Methylphenyl)ethylboronic acid (18). 46% yield from 1-(2-bromoethyl)-2-methylbenzene, m.p. $62\text{--}63^\circ\text{C}$. IR (KBr) $3600\text{--}3000$, 1371 , 1362 , 1227 , 784 cm^{-1} . ^1H NMR (DMSO- d_6) δ 0.85 (2H, t, $J = 8\text{ Hz}$), 2.22 (3H, s), 2.58 (2H, t, $J = 8\text{ Hz}$), $7.0\text{--}7.2$ (4H, m), 7.53 (2H, s, exchangeable with D_2O). ^{13}C NMR (DMSO- d_6) δ 16.1 (broad), 18.8 , 27.4 , 125.6 , 126.1 , 127.9 , 130.0 , 135.5 , 143.3 . HRMS 438.2734 (calcd for anhydride $\text{C}_{27}\text{H}_{33}\text{B}_3\text{O}_3$: 438.2709).

2-(3-Methylphenyl)ethylboronic acid (19). 45% yield from 1-(2-bromoethyl)-3-methylbenzene, m.p. $56\text{--}58^\circ\text{C}$. IR (KBr) $3600\text{--}3000$, 1373 , 1326 , 1222 , 781 , 760 cm^{-1} . ^1H NMR (DMSO- d_6) δ 0.89 (2H, t, $J = 8\text{ Hz}$), 2.23 (3H, s), 2.59 (2H, t, $J = 8\text{ Hz}$), $6.9\text{--}7.0$ (3H, m), $7.1\text{--}7.2$ (1H, m), 7.51 (2H, s, exchangeable with D_2O). ^{13}C NMR (DMSO- d_6) δ 17.2 (broad), 21.0 , 30.1 , 125.0 , 126.1 , 128.3 , 128.7 , 137.3 , 145.3 . HRMS 438.2714 (calcd for anhydride $\text{C}_{27}\text{H}_{33}\text{B}_3\text{O}_3$: 438.2709).

2-(4-Methylphenyl)ethylboronic acid (20). 50% yield from 1-(2-bromoethyl)-4-methylbenzene, m.p. 90–91 °C. IR (KBr) 3600–3000, 1376, 1025, 762 cm⁻¹. ¹H NMR (DMSO-d₆) δ 0.89 (2H, t, *J* = 8 Hz), 2.23 (3H, s), 2.59 (2H, t, *J* = 8 Hz), 6.9–7.2 (4H, m), 7.50 (2H, s, exchangeable with D₂O). ¹³C NMR (DMSO-d₆) δ 17.6 (broad), 20.6, 29.8, 127.9, 129.0, 134.3, 142.3. HRMS 438.2735 (calcd for anhydride C₂₇H₃₃B₃O₃: 438.2709).

2-(2-Methoxyphenyl)ethylboronic acid (21). 41% yield from 1-(2-bromoethyl)-2-methoxybenzene, m.p. 128–130 °C. IR (KBr) 3600–3000, 1377, 1028, 752 cm⁻¹. ¹H NMR (DMSO-d₆) δ 0.85 (2H, t, *J* = 8 Hz), 2.58 (2H, t, *J* = 8 Hz), 3.74 (3H, s), 6.8–7.2 (4H, m), 7.45 (2H, s, exchangeable with D₂O). ¹³C NMR (DMSO-d₆) δ 15.6 (broad), 24.4, 55.2, 110.6, 120.4, 126.7, 128.8, 133.2, 157.3. HRMS 486.2562 (calcd for anhydride C₂₇H₃₃B₃O₆: 486.2556).

2-(3-Methoxyphenyl)ethylboronic acid (22). 31% yield from 1-(2-bromoethyl)-3-methoxybenzene, m.p. 133–134 °C. IR (KBr) 3600–3000, 1490, 1396, 1260, 787 cm⁻¹. ¹H NMR (DMSO-d₆) δ 0.91 (2H, t, *J* = 8 Hz), 2.61 (2H, t, *J* = 8 Hz), 3.71 (3H, s), 6.6–7.2 (4H, m), 7.51 (2H, s, exchangeable with D₂O). ¹³C NMR (DMSO-d₆) δ 17.3 (broad), 30.3, 54.8, 110.8, 113.7, 120.3, 129.4, 147.1, 159.6. HRMS 486.2569 (calcd for anhydride C₂₇H₃₃B₃O₆: 486.2556).

2-(4-Methoxyphenyl)ethylboronic acid (23). 44% yield from 1-(2-bromoethyl)-4-methoxybenzene, m.p. 120–122 °C. IR (KBr) 3600–3000, 1377, 1039, 695 cm⁻¹. ¹H NMR (DMSO-d₆) δ 0.87 (2H, t, *J* = 8 Hz), 2.56 (2H, t, *J* = 8 Hz), 3.69 (3H, s), 6.80 (2H, d, *J* = 8 Hz), 7.08 (2H, d, *J* = 8 Hz), 7.48 (2H, s, exchangeable with D₂O). ¹³C NMR (DMSO-d₆) δ 18.0 (broad), 29.2, 55.0, 113.8, 128.9, 137.3, 157.2. HRMS 486.2560 (calcd for anhydride C₂₇H₃₃B₃O₆: 486.2556).

2-(4-Fluorophenyl)ethylboronic acid (24). 41 % yield from 1-(2-bromoethyl)-4-fluorobenzene, m.p. 50–52 °C. ¹H NMR (DMSO-d₆) δ 0.88 (2H, t, *J* = 8.2 Hz), 2.60 (2H, t, *J* = 8.2 Hz), 7.00–7.23 (4H, m), 7.52 (2H, s, exchangeable with D₂O). ¹³C NMR (DMSO-d₆) δ 17.6 (broad), 29.4, 115.0 (d, *J* = 20.8 Hz), 129.6 (d, *J* = 7.7 Hz), 141.5 (d, *J* = 3.1 Hz), 160.8 (d, *J* = 241.8). HRMS 450.1971 (calcd for anhydride C₂₄H₂₄B₃F₃O₃: 450.1957).

2-(2-Chlorophenyl)ethylboronic acid (25). 39% yield from 1-(2-bromoethyl)-2-chlorobenzene, m.p. 90–91 °C. IR (KBr) 3600–3000, 1551, 1252, 1005, 816 cm⁻¹. ¹H NMR (DMSO-d₆) δ 0.90 (2H, t, *J* = 8 Hz), 2.71 (2H, t, *J* = 8 Hz), 7.1–7.4 (4H, m), 7.58 (2H, s, exchangeable with D₂O). ¹³C NMR (DMSO-d₆) δ 15.5 (broad), 28.0, 127.5, 129.3, 130.0, 133.0, 142.6. HRMS 184.0458 (calcd for C₈H₁₀BClO₂: 184.0462), 498.1071 (calcd for anhydride C₂₄H₂₄B₃Cl₃O₃: 498.1070).

2-(3-Chlorophenyl)ethylboronic acid (26). 58% yield from 1-(2-bromoethyl)-3-chlorobenzene, m.p. 93–94 °C. IR

(KBr) 3600–3000, 1552, 1250, 1004, 795 cm⁻¹. ¹H NMR (DMSO-d₆) δ 0.89 (2H, t, *J* = 8 Hz), 2.66 (2H, t, *J* = 8 Hz), 7.1–7.3 (4H, m), 7.60 (2H, s, exchangeable with D₂O). ¹³C NMR (DMSO-d₆) δ 17.0 (broad), 29.8, 125.5, 126.8, 127.9, 130.6, 133.1, 148.0. HRMS 498.1071 (calcd for anhydride C₂₄H₂₄B₃Cl₃O₃: 498.1070).

2-(4-Chlorophenyl)ethylboronic acid (27). 62% yield from 1-(2-bromoethyl)-4-chlorobenzene, m.p. 90–91 °C. IR (KBr) 3600–3000, 1377, 1039, 695 cm⁻¹. ¹H NMR (DMSO-d₆) δ 0.88 (2H, t, *J* = 8 Hz), 2.60 (2H, t, *J* = 8 Hz), 7.18 (2H, d, *J* = 8 Hz), 7.28 (2H, d, *J* = 8 Hz), 7.58 (2H, s, exchangeable with D₂O). ¹³C NMR (DMSO-d₆) δ 17.4 (broad), 29.5, 128.3, 129.9, 130.1, 144.4. HRMS 184.0458 (calcd for C₈H₁₀BClO₂: 184.0462), 498.1071 (calcd for anhydride C₂₄H₂₄B₃Cl₃O₃: 498.1070).

2-(4-Trifluoromethylphenyl)ethylboronic acid (28). 66% yield from 1-(2-bromoethyl)-4-chlorobenzene, m.p. 88–89 °C. IR (KBr) 3600–3000, 1601, 1372, 1323, 1168, 1125, 1066, 784 cm⁻¹. ¹H NMR (DMSO-d₆) δ 0.91 (2H, t, *J* = 8 Hz), 2.70 (2H, t, *J* = 8 Hz), 7.39 (2H, d, *J* = 8 Hz), 7.60 (2H, d, *J* = 8 Hz), 7.62 (2H, s, exchangeable with D₂O). ¹³C NMR (DMSO-d₆) δ 17.1 (broad), 30.0, 125.2, 125.3, 138.8, 150.4. HRMS 218.0724 (calcd for anhydride C₉H₁₀BF₃O₂: 218.0726).

3-Phenylpropylboronic acid (29). 79% yield from 1-bromo-3-phenylpropane, m.p. 78–80 °C. IR (KBr) 3600–3000, 1377, 1039, 695 cm⁻¹. ¹H NMR (DMSO-d₆) δ 0.60 (2H, t, *J* = 8 Hz), 1.55–1.65 (2H, m), 2.51 (2H, t, *J* = 8 Hz), 7.1–7.3 (5H, m), 7.42 (2H, s, exchangeable with D₂O). ¹³C NMR (DMSO-d₆) δ 14.6 (broad), 26.2, 38.5, 126.2, 128.7, 128.9, 142.8. HRMS 438.2725 (calcd for anhydride C₂₇H₃₃B₃O₃: 438.2709).

2-(1-Naphthyl)ethylboronic acid (30). 38% yield from 1-(2-bromoethyl)-1-naphthalene, m.p. 65–68 °C. IR (KBr) 3600–3000, 1377, 1039, 695 cm⁻¹. ¹H NMR (DMSO-d₆) δ 1.05 (2H, t, *J* = 8 Hz), 3.11 (2H, t, *J* = 8 Hz), 7.3–8.2 (7H, m), 7.65 (2H, s, exchangeable with D₂O). ¹³C NMR (DMSO-d₆) δ 16.9 (broad), 27.2, 124.1, 125.0, 125.7, 126.0, 126.2, 128.8, 131.6, 133.8, 141.5. HRMS 546.2718 (calcd for anhydride C₃₆H₃₃B₃O₃: 546.2709).

2-(2-Naphthyl)ethylboronic acid (31). 25% yield from 1-(2-bromoethyl)-2-naphthalene, m.p. 136–137 °C. IR (KBr) 3600–3000, 1377, 1039, 695 cm⁻¹. ¹H NMR (DMSO-d₆) δ 1.01 (2H, t, *J* = 8 Hz), 2.81 (2H, t, *J* = 8 Hz), 7.3–7.9 (7H, m), 7.57 (2H, s, exchangeable with D₂O). ¹³C NMR (DMSO-d₆) δ 18.5 (broad), 30.4, 125.2, 125.4, 126.1, 127.5, 127.6, 127.7, 127.8, 131.8, 133.6, 143.1. HRMS 546.2727 (calcd for anhydride C₃₆H₃₃B₃O₃: 546.2709).

2-(4-Carboxyphenyl)ethyl boronic acid (32). To a solution of methyl-4-hydroxybenzoate (4.49 g, 29.5 mmol) in pyridine (25 mL) containing DMAP (2 mol%, 72 mg, 0.59 mmol) cooled with an ice bath, was added triflic anhydride (10.0 g, 35.4 mmol). The solution was refluxed for 72 h, then poured into water (100 mL) and extracted

with diethyl ether (3 x 50 mL). The combined organic layers were successively washed with water (50 mL), 1 M hydrochloric acid (3 x 50 mL), water (50 mL) and brine (50 mL). After drying (MgSO_4), and evaporation, the residue was flash chromatographed (hexanes:ethyl acetate (10:1) elution) to give methyl-4-trifluoroacetoxybenzoate (**34**) as a clear colorless oil (7.04 g, 84% yield); IR (film) 1736, 1609, 885 cm^{-1} ; ^1H NMR (CDCl_3) δ 3.92 (3H, s), 7.33 (2H, dd, $J_o = 9$ Hz, $J_m = 2$ Hz), 8.13 (2H, dd, $J_o = 9$ Hz, $J_m = 2$ Hz). ^{13}C NMR (CDCl_3) δ 52.47, 118.72, 121.41, 130.38, 131.87, 152.48, 165.36. HRMS 283.9953 (calcd for $\text{C}_9\text{H}_7\text{F}_3\text{O}_5\text{S}$: 283.9966).

To a solution of methyl-4-trifluoroacetoxybenzoate (**34**, 5.14 g, 18.1 mmol) in 1,4-dioxane (90 mL) were added tetravinyltin (3.4 mL, 18.7 mmol), lithium chloride (2.3 g, 54.3 mmol), tetrakis(triphenylphosphine) palladium(0) (5 g, 4.3 mmol) and a few crystals of 2,6-di-*tert*-butyl-4-methyl phenol. The resulting suspension was heated under reflux for 24 h, then cooled to 20 °C and treated with pyridine (10 mL) and pyridinium fluoride (2 mL of a 1.4 M solution in THF, 28 mmol). The resulting mixture was stirred at 25 °C for 16 h. The reaction mixture was then diluted with diethyl ether (100 mL), filtered through Celite and washed successively with water (75 mL), 10% hydrochloric acid (75 mL), water (75 mL) and brine (75 mL). The solution was dried (MgSO_4), concentrated, and flash chromatographed (hexanes:ethyl acetate (50:1) elution) to yield methyl-4-vinylbenzoate (**35**, 1.88 g, 64%) m.p. 31–32 °C; IR (KBr) 1724, 1607 cm^{-1} . ^1H NMR (CDCl_3) δ 3.89 (3H, s), 5.36 (1H, d, $J_{cis} = 11$ Hz), 5.84 (1H, d, $J_{trans} = 18$ Hz), 6.73 (1H, dd, $J_{cis} = 11$ Hz, $J_{trans} = 18$ Hz), 7.44 (2H, dd, $J_o = 9$ Hz, $J_m = 2$ Hz), 7.98 (2H, dd, $J_o = 9$ Hz, $J_m = 2$ Hz). ^{13}C NMR (CDCl_3) δ 52.12, 116.50, 126.13, 129.29, 129.90, 136.03, 141.93, 166.86. HRMS 162.0695 (calcd for $\text{C}_{10}\text{H}_{10}\text{O}_2$: 162.0681).

Dibromoborane–dimethyl sulfide complex (7.27 mL of a 1 M solution in CH_2Cl_2 7.27 mmol) was added to neat methyl 4-vinylbenzoate (**35**, 1.1792 g, 7.27 mmol) under argon, and the resulting mixture heated under reflux overnight. The reaction was then quenched with ice–water mixture (100 mL) and extracted with diethyl ether (3 x 50 mL). The combined fractions were extracted with 10% aqueous NaOH (3 x 50 mL), acidified with conc. hydrochloric acid and extracted with diethyl ether (3 x 75 mL). Water (10 mL) was then added to the ether extracts and the mixture evaporated under reduced pressure at < 30 °C until the boronic acid precipitated. The mixture was then cooled at 5 °C overnight and the boronic acid was collected by vacuum filtration, washed with cold water (3 x 5 mL) and air dried to yield 2-(4-carboxyphenyl)ethyl boronic acid (**32**, 0.32 g, 21%) as the monohydrate, m.p. 130–138 °C. IR (KBr) 3600–2400, 1675, 1610, 1430–1280, 1181, 1121, 846, 770 cm^{-1} . ^1H NMR ($\text{DMSO}-d_6$) δ 0.91 (2H, t, $J = 8.0$ Hz), 2.68 (2H, t, $J = 8.0$ Hz), 3.35 (2H, s), 7.28 (2H, d, $J = 8.0$ Hz), 7.57, (2H, s), 7.82 (2H, d, $J = 8.0$ Hz), 12.77 (1H, s). ^{13}C NMR ($\text{DMSO}-d_6$) δ 17.6, 30.5, 125.7, 127.9, 150.5, 167.3. HRMS 176.0631 (calcd for $\text{C}_9\text{H}_{11}\text{BO}_4\cdot\text{H}_2\text{O}$ 176.0645).

Computational Methods

System setup

The reference structure used was that of the subtilisin Carlsberg crystal structure of McPhalen and James⁶ available from the Protein Data Bank²⁸ at Brookhaven National Laboratory.²⁹ The setup was done with INSIGHT II, version 2.0.0 (Biosym Technologies, Inc., San Diego, CA, U.S.A.). To create initial coordinates for the minimization, the inhibitor (eglin C) and the three calcium ions were removed. Hydrogens were added at the pH used for the kinetic measurements (pH 7.8). This protonated all Lys, Arg, His residues, and the N-terminus, and deprotonated the acids Glu, Asp and the C-terminus. In the calculations of the boronic acid–enzyme complexes, a tetrahedral carbon atom was used to mimic the boron atom since, as yet, no forcefield parameters have been reported for boron. This approximation was considered acceptable since only energy differences resulting from changes remote from boron were being explored. To set up the initial structure for the energy minimization the boron-equivalent carbon was covalently bound to O of the hydroxyl group of the active site serine 221. The X-ray structure of 2-phenethylboronic acid (**17**) bound to subtilisin BPN^{12a} was used as the model to guide dockings of the substituted 2-phenethylboronic acids of Table 2 into the active site of subtilisin Carlsberg. The two hydroxy groups attached to the boron were oriented such that one pointed to Asp155 of the oxyanion hole and the other to His64, which becomes positively charged after the addition of the proton from Ser221. The aromatic residue of each inhibitor was positioned in the S_1 pocket in a manner that avoided all bad Van der Waals interactions. Charges on Ser221 and the enzyme-bound boronic acid were generated by AM1 calculations (MOPAC 6.0) and scaled to fit those of the CVFF library. The overall negative charge of -1 was mostly on, and distributed between, the oxygen atoms bound to boron. The boron atom itself was assigned a charge of -0.01. This model system was solvated in a rectangular box (49 x 47 x 49 Å³) of water molecules. The total number of water molecules in this system was 2318. The overall charge of the enzyme–inhibitor complex resulting from this setup was -1.

Energy minimization

The simulations were performed with the DISCOVER program, Version 2.7.0 (Biosym Technologies, Inc., San Diego, CA, U.S.A.) on a Silicon Graphics 240 GTX computer, using the Consistent Valence Force Field (CVFF).³⁰ A non-bonded cutoff of 10 Å with a switching function between 7.5 and 9 Å was used. The non-bonded pair list was updated every 20 cycles and a dielectric constant of 1 was used in all calculations. The energy of the system was minimized with respect to all 3N Cartesian coordinates until the maximum derivative of 0.1 kcal mol⁻¹ Å⁻¹ was reached. The resulting structure was used as the starting point for the molecular dynamics calculations. During the molecular dynamics simulations, the whole enzyme, with the exception of a 12 Å radius region around

Ser221, was kept fixed, as were water atoms more than 15 Å away from Ser221. The MD simulations were performed for 20 ps with an initial equilibrium period of 10 ps and a timestep 10 fs.

Electrostatic mapping of the S₁ pocket

The calculations were performed with DelPhi, version 2.2.0 (Biosym Technologies, Inc., San Diego, CA, U.S.A.). The previously obtained (see above) Discover-minimized coordinates of enzyme and enzyme-inhibitor complex were used. The S₁ pocket was defined by Ser125-Ala129, Ala152-Gly154, Ile165-Tyr167, and only these residues were included for the enzyme calculations. El-complex calculations involved the *para*-Cl-PheCH₂CH₂ group of 27 in addition to the above S₁-amino acid residues. The charges were obtained by single-point AM1 calculations on total valence satisfied atoms of the enzyme sub-sets defined above. The NH, CO and CH₂ groups artificially created when the above sub-sets were "split-off" from the full enzyme structure were converted into NH₂, COH and CH₃ respectively, wherever necessary. The Van der Waals radii supplied with the CVFF force field and a dielectric constant of 1 were used in all calculations.

Kinetic measurements

The reference substrate used was *N*-*para*-tosyl-L-arginine methyl ester (TAME), with initial rates of subtilisin-catalyzed hydrolyses being determined by NaOH solution titrations using a pH-stat.³ All rates were determined at 25 °C on reaction mixtures containing aqueous 1 M KCl (1 mL), an aliquot (0.4, 0.6, 0.8, 1.0, 2.0, 4.0, 8.0 mL) of 0.37 M aqueous TAME solution and saturated aqueous inhibitor solution (1×10^{-5} – 1×10^{-2} M). In each case water was added to bring the final volume to 10 mL to give final concentrations of 0.015–0.30 M of substrate and 10^{-6} – 10^{-3} M of inhibitor. Actual boronic acid concentrations in all stock solutions were established by titration with 0.02 M NaOH solution. After equilibration for 5 min, the pH of the assay cell was adjusted to 7.8 with 0.2 M NaOH and the reaction initiated by addition of 50 µL of subtilisin Carlsberg stock solution (7.33×10^{-5} M in 0.1 M phosphate buffer pH 7.8). The rate of uptake of 0.2 M NaOH was recorded directly into a PC and *K*_i's were determined using the Grafit program (Erithacus Software Ltd, U.K.). All kinetic runs were performed in duplicate at two different concentrations of boronic acid. The results are recorded in Tables 1 and 2.

Acknowledgements

Support from the Natural Sciences and Engineering Research Council of Canada is gratefully acknowledged. We also thank the Fonds zur Förderung der wissenschaftlichen Forschung, Vienna, for a postdoctoral scholarship award (to P. S.-W.) and Professor H. Hönig (Graz) for a gift of 3-chloro- and 3,5-di-chloro-phenylboronic acids.

References and Notes

- (a) In *Preparative Biotransformations*, Roberts, S. M., Ed.; Wiley: NY, 1993; (b) Sih, C. J.; Gu, Q.-M.; Holdrun, X.; Harris, K. *Chirality* **1992**, *4*, 91–97; (c) In *Biotransformations in Preparative Organic Chemistry*, Faber, K., Ed.; Springer-Verlag: Heidelberg, 1992; (d) Santaniello, E.; Ferraboschi, P.; Grisenti, P.; Manzocchi, A. *Chem. Rev.* **1992**, *92*, 1071–1140; (e) Boland, W.; Froessl, C.; Lorenz, M. *Synthesis* **1991**, 1049–1072; (f) Davies, H. G.; Green, R. H.; Kelly, D. R.; Roberts, S. M. In *Biotransformations in Preparative Organic Chemistry*, Academic Press: London, 1990; (g) Klibanov, A. M. *Acc. Chem. Res.* **1990**, *23*, 114–120; (h) Jones, J. B. *Tetrahedron* **1986**, *42*, 3351–3403.
- Philipp, M.; Bender, M. L. *Molec. Cell. Biochem.* **1983**, *51*, 5–32.
- Bonneau, P. R.; Graycar, T. P.; Estell, D. A.; Jones, J. B. *J. Am. Chem. Soc.* **1991**, *113*, 1026–1030; and references cited therein.
- (a) In *Computer-Aided Drug Design*, Perun, T. J.; Probst, C. L., Eds.; Marcel-Dekker Inc.: NY, 1989; (b) In *Crystallographic and Modeling Methods in Molecular Design*, Bugg, D. E.; Ealick, S. E., Eds.; Springer-Verlag: Berlin, 1990.
- (a) Delinck, D. L.; Margolin, A. L. *Tetrahedron Lett.* **1990**, *31*, 3093–3096; (b) Pugniere, M.; San Juan, C.; Previero, A. *Tetrahedron Lett.* **1990**, *31*, 4883–4886; (c) Gotor, V.; Garcia, M. J.; Rebollo, F. *Tetrahedron: Asymmetry* **1990**, *1*, 277–278. (d) Margolin, A. L.; Delinck, D. L.; Whalon, M. R. *J. Am. Chem. Soc.* **1990**, *112*, 2849–2854. (e) Chenevert, R.; Desjardins, M.; Gagnon, R. *Chem. Lett.* **1990**, 33–34; (f) Chenevert, R.; Letourneau, M.; Thiboutot, S. *Can. J. Chem.* **1990**, 960–963.
- McPhalen, C. A.; James M. N. G. *Biochemistry* **1988**, *27*, 6582–6598.
- (a) Wong, C.-H.; Chen, S.-T.; Hennen, W. J.; Bibbs, J. A.; Wang, Y. F.; Liu, J. L.-C.; Pantoliano, M. W.; Whitlow, M.; Bryan, P. N. *J. Am. Chem. Soc.* **1990**, *112*, 945–953; (b) Karasaki, Y.; Ohno, M. *J. Biochem.* **1979**, *86*, 536–537; (c) Karasaki, Y.; Ohno, M. *J. Biochem.* **1978**, *84*, 531–538; (d) Williams, A.; Woolford, G. *J. Chem. Soc., Perkin Trans. II* **1972**, 272–275.
- (a) Schechter, I.; Berger, A. *Biochem. Biophys. Res. Commun.* **1967**, *27*, 157–162; (b) Berger, A.; Schechter, I. *Phil. Trans. R. Soc. Lond., Ser. B* **1970**, *257*, 249–264.
- (a) Elgendy, S.; Deadman, J.; Patel, G.; Green, D.; Chino, N.; Goodwin, C. A.; Scully, M. F.; Kakkar, V. V.; Claeson, G. *Tetrahedron Lett.* **1992**, *33*, 4209–4212; (b) Kettner, C.; Mersinger, L.; Knaubb, R. *J. Biol. Chem.* **1990**, *265*, 18289–18297; (c) Abouakil, N.; Lombardo, D. *Biochim. Biophys. Acta* **1989**, *1004*, 215–220; (d) Crompton, I. E.; Cuthbert, B. K.; Lowe, C.; Waley, S. G. *Biochem. J.* **1988**, *251*, 453–459; (e) Goz, B.; Ganguli, C.; Troconis, M.; Wyrick, S.; Isahq, K. S.; Katzenellenbogen, J. A. *Biochem. Pharm.* **1986**, *35*, 3587–3591; (f) Kettner, C. A.; Shenvi, A. B. *J. Biol. Chem.* **1984**, *259*, 15106–15114; (g) Tsai, I. H.; Bender, M. L. *Arch. Biochem. Biophys.* **1984**, *228*, 555–559; (h) Matteson, D. S.; Sadhu, K. M.; Lienhard, G. F. *J. Am. Chem. Soc.* **1981**, *103*, 5241–5242; (i) Garner, C. W. *J. Biol. Chem.* **1980**, *255*, 5064–5068; (j) Nakatani, H.; Uehara, Y.; Hiromi, K. *J. Biochem.* **1975**, *78*, 611–616; (k) Rawn, D.; Lienhardt, G. E. *Biochemistry* **1974**, *13*, 3124–3130; (l) Phillip, M.; Bender, M. L. *Proc. Natl Acad. Sci.*

- U.S.A. 1971, 68, 478–480; (m) Koehler, K. A.; Lienhardt, G. E. *Biochemistry* 1971, 10, 2477–2483; (n) Antonov, V. K.; Ivanina, T. V.; Berezin, I. V.; Martinek K. *FEBS Lett.* 1970, 7, 23–25.
10. Keller, T. H.; Seufer-Wasserthal, P.; Jones, J. B. *Biochem. Biophys. Res. Commun.* 1991, 176, 401–405.
11. (a) Matteson, D. S. In *The Chemistry of the Metal–Carbon Bond*, Vol. 4, p. 309, Wiley; NY, 1987; (b) Washburn, R. M.; Levens, E.; Albright, E. F.; Billing, F. A. In *Organic Synthesis*, Wiley; NY, 1963.
12. Washburn, R. M.; Billing, F. A.; Bloom, M.; Albright, C. F.; Levens, E. *Adv. Chem. Ser.* 1961, 32, 208–220.
13. Matteson, D. S.; Majumdar, D. *Organometallics* 1983, 2, 1529–1534.
14. Stille, J. K.; Echavarren, A. M. *J. Am. Chem. Soc.* 1987, 109, 5478–5486.
15. Brown, C. H.; Ravindran, N.; Kulkarni, S. U. *J. Org. Chem.* 1980, 45, 384–389.
16. For the determination of the pK_a 's, a saturated aqueous solution of each boronic acid was titrated with 0.02 M NaOH and the equivalence point obtained by using the first deviation of the titration curve.
17. Nakatani, H.; Morita, T.; Hiromi, K. *Biochim. Biophys. Acta* 1978, 525, 423–428.
18. (a) Wolfenden, R. *Science* 1983, 222, 1087–1093; (b) Wolfenden, R.; Kati, W. M. *Acc. Chem. Res.* 1991, 24, 209–215.
19. DelPhi User Guide, version 2.4. San Diego; Biosym Technologies, 1993.
20. (a) Hine, J.; Mookerjee, P. K. *J. Org. Chem.* 1975, 40, 292–298; (b) Cabani, S.; Gianni, P.; Mollica, V.; Lepori, V. *J. Solut. Chem.* 1981, 10, 563–595.
21. Rotanova, T. V.; Vasileva, T. V.; Ginodman, L. M.; Antonov, V. M. *Bioorg. Khim.* 1978, 4, 694–698.
22. Suzuki, S.; Green, P. G.; Bumgarner, R. E.; Dasgupta, S.; Goddard, III, W. A.; Blake, G. A. *Science* 1992, 257, 942–945.
23. (a) Gilson, M.; Honig, B. *Nature* 1987, 330, 84–86; (b) Lamotte-Brasseur, J.; Dive, G.; Dehareng, D.; Ghuysen, J. M. *J. Theor. Biol.* 1990, 145, 183–198.
24. The free energy of desolvation for benzoate was evaluated using DelPhi. Such a calculation requires two DelPhi runs with different solvent dielectric constants. The solvent dielectric is 1.0 (vacuum) in the first run, and it is the dielectric of the solvent (80.0) for water in the second. The solvation energy is then the total energy in solvent minus the total energy in vacuum. The found value is 72.5 kcal/mole.
25. Perrin, D. D.; Armarego, W. L. F.; Perrin, D. R. In *Purification of Laboratory Chemicals*, Pergamon Press; NY, 1980.
26. Since boronic acids form anhydrides very readily, the recorded melting points may well be those of the corresponding anhydrides in some cases. The ease with which anhydrides form also precluded accurate elemental analyses for the previously unknown boronic acids prepared.
27. Yabroff, D. L.; Branch, G. E.; Bettman, B. *J. Am. Chem. Soc.* 1934, 56, 1850–1857.
28. Entry 2SEC, version of January 1992, 1.8-Å resolution.
29. (a) Bernstein, F. C.; Koetzle, T. F.; Williams, J. B.; Meyer, Jr, E. F.; Brice, M. D.; Rodgers, J. R.; Kennard, O.; Shimanouchi, T.; Tasumi, M. *J. Mol. Biol.* 1977, 112, 535–542; (b) Abola, E. E.; Bernstein F. C.; Bryant, S. H.; Koetzle, T. F.; Weng, J. In *Crystallographic Databases — Information Content, Software Systems, Scientific Applications*, pp. 107–132, Allen, F. H.; Bergerhoff, G.; Sievers, R., Eds.; Data Commission of the International Union of Crystallography; Bonn, 1987.
30. Hagler, A. T.; Osguthorpe, D. J.; Dauber-Osguthorpe, P.; Hempel, J. C. *Science* 1985, 227, 1309–1315.

(Received 14 October 1993; accepted 9 November 1993)